Advanced Energy Systems and Intelligent Geoscience (AESIG)
https://www.mospbs.com/journal/aesig

• *Article* •

Numerical Simulation and Sensitivity Analysis of Key Parameters for Modified Silicon-Based Nanoparticle Enhanced Oil Recovery in Low-Permeability Reservoirs

Chen Zhang, Xiang Rao*

School of Petroleum Engineering, Yangtze University, Wuhan 430100, China

***Corresponding Author:** Xiang Rao **Email:** raoxiang0103@163.com

Received: 21 January 2026 **Accepted:** 26 January 2026

Abstract: To solve the low recovery rate of low-permeability heterogeneous reservoirs in mid-late oilfield development, this study focuses on modified silicon-based nanoparticle EOR technology (strong migration, good environmental compatibility). A 3D two-phase two-component model was built via CMG-STARS (single-well homogeneous & single-injection four-production heterogeneous scenarios). Sensitivity analysis of 5 key parameters (injection concentration/rate/timing, reservoir permeability/porosity) was conducted by orthogonal tests. Results: Optimal parameters raise cumulative recovery to 65.8% (13.6 pts higher than water flooding); high-permeability/porosity reservoirs perform better; nanoparticle plugging increases low-permeability zone recovery by 10.2% in heterogeneous reservoirs. This work quantifies the coupling mechanism between injection parameters and reservoir properties, advances the simulation system, and supports on-site injection scheme design.

Keywords: Nanoparticle-enhanced oil recovery; Numerical simulation; CMG-STARS; Parameter sensitivity analysis; Heterogeneous reservoir; Reservoir simulation

Glossary

ORF	Oil Recovery Factor
EOR	Enhanced oil recovery
IFT	Interfacial tension
OOIP	Original oil in place
σ	Interfacial Tension
θ	Contact Angle

1 Introduction

In the global energy system, the dominant position of oil as a primary energy source is irreplaceable in the short term. The International Energy Agency (IEA) predicts that driven by the development of emerging economies, global oil demand will continue to grow in the next few decades (Ackah and Kizys, 2015). However, Long-term high-intensity exploitation has pushed major global oilfields into mid-late development, with challenges like pressure depletion and low recovery (conventional crude: 30%-40%). Low-permeability reservoirs (<10false) account for 30.9% of China's new reserves; their micro-pores and

DOI: https://doi.org/10.58244/aesig.263533

high seepage resistance restrict water flooding recovery to 15%-25%, a key bottleneck for stable production (Li et al., 2025). Against this backdrop, nanoparticle-based Enhanced Oil Recovery (EOR) technology, as an emerging tertiary oil recovery method with significant potential for enhanced recovery, has become a research hotspot in the energy field (Agista et al., 2018).

Nanoparticles have unique small-size, surface, and quantum size effects, which give them irreplaceable advantages over traditional oil displacement agents in improving displacement fluid properties and regulating reservoir micro-seepage characteristics (Agi et al., 2018). The mechanisms by which nanoparticles enhance oil recovery mainly include: (1) Increasing fluid viscosity: Enhancing cohesion through interactions with displacement fluid molecules to optimize the mobility ratio, reduce fingering, and expand sweep volume; (2) Reducing oil-water interfacial tension (IFT): Adsorbing on the interface via a high specific surface area to alter interface properties, promoting oil droplet detachment and improving oil washing efficiency; (3) Modifying rock wettability: Adjusting surface properties through the adsorption of hydrophilic or lipophilic particles to optimize displacement effects; (4) Plugging high-permeability channels: Preferentially entering and accumulating in high-permeability pores in heterogeneous reservoirs to force fluids to divert to low-permeability zones, thereby improving sweep efficiency (Druetta and Picchioni, 2019). Research on nanoparticle EOR technology has a long history and has achieved a series of important results.

In terms of mechanism research, Lv et al. (2023) found that nanoparticle oil displacement agents exhibit excellent profile control performance, effectively plugging high-permeability channels and forcing displacement fluids to divert to low-oil-content zones. Singh and Mohanty (2015) studied silica nanoparticle-anionic surfactant synergy via static foam tests, fluorescence microscopy, and core displacement. Low-concentration (0.3 wt.%) nanoparticles enhanced foam stability, doubled mobility reduction factor, and the composite system's immiscible foam flooding boosted oil recovery by ~10% vs water flooding, strengthening surfactants' subsurface foam-stabilizing ability.

El-Diasty and Aly (2015) proposed a theoretical model to predict the migration behaviour of nanoparticles in porous media, comprehensively considering factors such as pore structure, fluid flow rate, and nanoparticle surface charge, providing an accurate theoretical basis for understanding migration mechanisms. Numerical simulation is a promising tool for reservoir flow problems, with a wealth of advanced numerical methods and models having been continuously proposed and improved for more accurate and efficient simulation of reservoir seepage characteristics (Rao et al., 2022; Rao et al., 2023a; Rao et al., 2024a; Li et al., 2025; Zhang et al., 2025; Rao et al., 2023b; Rao et al., 2024b). Numerous research teams, including Lu and Zhang (2017), Khalilnezhad et al. (2023), Mohanty et al. (2021), Khoramian et al. (2019), and Yang et al. (2022), have systematically studied the effects of various nanoparticles (e.g., silica, alumina, zinc oxide) on oil displacement performance through a large number of laboratory experiments. They confirmed that nanoparticle composite polymer systems can increase oil recovery by 4.48%-10.33%, with some systems achieving increases of 10%-20% and maintaining good stability under high-temperature and high-salinity conditions. Chen et al. (2025), used advanced characterization techniques to deeply explore the stability and dispersibility of nanoparticles in reservoir environments, as well as their interaction mechanisms

with asphaltenes and resins in crude oil, clarifying the specific pathways for improving crude oil fluidity. Guzei et al. (2022), constructed a 2D micromodel using the VOF method and combined it with physicochemical property tests of SiO_2 nanofluids to investigate their oil displacement effects on different lithology reservoirs. Sepehri et al. (2019) focused on lithology differences via numerical modelling: carbonate reservoirs benefit more from nanoparticle-induced wettability alteration than sandstone under the same injection. A 1 wt.% nanofluid boosted dolomite/sandstone recovery by 39% and basalt by 89% vs water flooding; enhancement is more significant under low capillary number and low-viscosity oil. Zhang, Li, and Wang (2019), further validated the wettability alteration mechanism via combined micromodel experiments and CFD simulations, revealing that silica nanoparticles effectively modify the oil-wet glass surface to water-wet, leading to a 13% increase in oil recovery rate in numerical simulations and a 9% enhancement in experimental tests. Ivanov et al. (2025), conducted a systematic microfluidic study on the use of diluted silica sols for enhanced oil displacement, providing direct visual evidence for the pore-scale oil displacement mechanism of silica-based nanoparticles.

In terms of numerical simulation research, Cao. (2015), developed an internal simulator to simulate the transport of hydrophilic nanofluids in porous media, verified by commercial software, and analysed the oil displacement effects of different injection strategies, with continuous injection increasing the maximum recovery rate to 77% compared to water flooding. Ortiz Maestre and Daza (2017), established a mechanistic model of nanoparticle-stabilized supercritical CO_2 foam based on experimental data and performed 2D simulation of the Lisama oilfield in Colombia using CMG-STARS, confirming that this system improves recovery by 10%-15% compared to gas-water co-injection. Kumar, Pal, and Mandal (2021), studied the oil displacement performance of nanoemulsion flooding through CMG-STARS numerical simulation and history matching, achieving a tertiary recovery rate of 28.32% (Original Oil In Place, OOIP), which is approximately 3 percentage points higher than that of a single surfactant system. Mahmud et al. (2021), used CMG-STARS to construct a 3D model to simulate SiO_2-SDS flooding in sandstone reservoirs. After verification with experimental data (error < 5%), they determined that the recovery rate reaches 75.5% at a concentration of 0.15 wt.% and an injection rate of 2 mL/min. Jafarbeigi et al. (2022) used lab experiments and numerical simulation to study the 3:1 SiO_2-ZnO composite nanofluid's oil displacement performance. In sandstone cores, 0.2 wt.% of this system improved efficiency by 8.5 pts vs single SiO_2 (recovery: 70.2%). Simulation verified this, confirming the composite system enhances rock wettability (contact angle: 120° oil-wet to 65° weakly water-wet) and optimizes nanoparticle migration, reducing pore plugging risk. Shao et al. (2023) explored nanofluids' oil displacement mechanism/performance in porous media via spontaneous imbibition tests, contact angle measurements, CMG simulation, and mechanism analysis. Modified SiO_2's spontaneous imbibition recovery reached 38.8% (11.5% higher than unmodified particles, 25% vs brine flooding). The 0.1 wt.% AOS + 0.2 wt.% SiO_2 composite system achieved 42.1% recovery (6.5 pts higher than single surfactant), showing nanoparticle-surfactant synergy. Bahadori et al. (2024) explored surfactant-silica nanoparticle synergistic oil displacement via pendant drop (dynamic IFT), contact angle (wettability), and COMSOL (microscale droplet simulation). Triton X-100 reduced

IFT, SiO_2 improved rock hydrophilicity; gel treatment delayed tracer breakthrough (25→240 h), expanding sweep volume. Garcia et al. (2025), conducted a numerical study on the mechanisms of nano-assisted foam flooding in porous media as an alternative to gas flooding, providing new insights for the application of nanoparticle technology in gas-based EOR. Wang et al. (2024), carried out a comprehensive study of nano-composite polymer flooding under reservoir conditions, providing new insights into enhanced oil recovery.

Although existing studies have confirmed the feasibility and application potential of nanoparticle EOR technology in enhancing recovery from both mechanism verification and numerical simulation perspectives, the current research system still has obvious gaps targeting modified silicon-based nanoparticles in low-permeability reservoirs: (1) Most studies focus on single-well homogeneous models, neglecting multi-well heterogeneous conditions common in actual low-permeability oilfields—especially the regulatory effects of inter-well permeability differences and well pattern interference on modified silicon-based nanoparticles' oil displacement efficiency (Ivanov et al., 2025; Li et al., 2025); (2) Core parameter optimization (injection concentration, timing, etc.) mostly relies on single-variable analysis, failing to reveal parameter interactions (e.g., concentration-permeability-rate) or fully verify optimal combinations' applicability in complex multi-well low-permeability scenarios (Chen et al., 2025; Wang et al., 2024); (3) Existing studies lack accurate quantitative explanation of how too low modified silicon-based nanoparticle concentrations fail to exert interface regulation/plugging effects, while excessive concentrations cause aggregation and pore plugging in low-permeability reservoirs—hindering on-site injection scheme design (Shao et al., 2023; Khoramian et al., 2019).

Based on this, the core goal of this study is to address the above research gaps. We constructed multi-scenario numerical models of modified silicon-based nanoparticle EOR, including single-well homogeneous and single-injection four-production heterogeneous models, systematically analysed the influence laws and parameter interaction effects of injection parameters (concentration, rate, timing) and reservoir physical parameters (permeability, porosity) on recovery rate, quantified the regulatory mechanism of inter-well permeability differences in heterogeneous low-permeability reservoirs, improved the numerical simulation method system of modified silicon-based nanoparticle EOR technology, and provided scientific and reliable theoretical support for the on-site promotion and application of this technology and the optimization of injection schemes.

2 Methods

The CMG-STARS module is capable of simulating multi-component and multi-phase flow, supporting the integration of chemical reaction models, and establishing phase equilibrium equations tailored to diverse geological conditions. To ensure the reliability and reproducibility of the numerical simulation, all experimental and modelling procedures in this study strictly adhere to relevant industry standards (e.g., ASTM D7370 for core flooding, ASTM D2855 for porosity measurement). Based on this, a 3D two-phase two-component numerical model for modified silicon-based nanoparticle EOR was established using CMG-STARS.

2.1 Model assumptions

To simplify the numerical simulation while focusing on the core mechanism of nanoparticle-enhanced oil recovery, the following basic assumptions were proposed for the reservoir

model, with references to existing mature simulation frameworks (El-Amin and Mahmoud, 2014; Mahmud et al., 2021). Reservoir fluids consist of two immiscible phases (oil and water), with no chemical reactions between nanoparticles and reservoir rocks/fluids—nanoparticles act on oil displacement solely via physical effects (pore plugging, wettability modification, interfacial tension reduction). The rock matrix is assumed incompressible: porosity and permeability are isotropic in homogeneous models, while permeability anisotropy in heterogeneous models is characterized by a permeability correction factor. Fluid flow adheres to Darcy's law (inertial forces neglected due to low-velocity seepage in low-permeability reservoirs), and the oil-water interfacial tension coefficient is treated as a temperature/pressure-independent constant, consistent with ASTM D7370 experimental conditions.

2.2 Mass conservation equation

The mass conservation equation for single-phase flow is:

$$\frac{\partial(\rho\varphi)}{\partial t}+\nabla\cdot(\rho u)=\rho q \tag{1}$$

where φ is the rock porosity, dimensionless parameter; ρ is the fluid density, $\mathrm{kg/m^3}$; u is the fluid velocity, $\mathrm{m/s}$; q represents the source/sink term, $\mathrm{s^{-1}}$.

The velocity in Equation (8) is given by Darcy's law:

$$u=-\frac{k}{\mu}(\nabla p-\rho g\nabla z) \tag{2}$$

where k is the absolute permeability, mD; μ is the fluid viscosity, $\mathrm{Pa\cdot s}$; p is the pressure, Pa; g is the gravitational acceleration, $\mathrm{m/s^2}$; z is the vertically downward coordinate, m; Darcy's law is equivalent to the momentum conservation equation.

2.3 Phase equilibrium equation

In the three-dimensional two-phase two-component numerical model for nanoparticle-enhanced oil recovery (EOR), the core of phase equilibrium lies in describing the distribution law of crude oil components and water between the oil phase and aqueous phase, while considering the regulatory effect of nanoparticles on phase interfacial behaviour (such as reducing interfacial tension and altering wettability). Based on the phase equilibrium calculation logic of the CMG-STARS simulator and combined with thermodynamic theoretical derivation, the phase equilibrium equation system is as follows:

2.3.1 K-value correlation considering temperature and pressure effects

Actual reservoirs are non-ideal systems, where the K is significantly affected by temperature (T) and pressure (P). The simplified correlation derived from the Clausius-Clapeyron equation is as follows:

$$K_i^{ow}=(p,T)=\frac{a_i}{p}\cdot\exp\left(-\frac{b_i}{T}\right)\cdot f(c) \tag{3}$$

$$a_i=p_{vi}(T_1)\cdot\exp\left(\frac{b_i}{T_1}\right),\ b_i=\frac{\Delta H_i}{R} \tag{4}$$

where $p_{vi}(T_1)$ is the pure-component vapor pressure of component i, Pa; ΔH_i is the enthalpy of vaporization of component i, $\mathrm{J/mol}$; R is the universal gas constant, $8.314\mathrm{J/mol\cdot K}$; T_1 is the reference temperature, K.

$f(c)$ is the nanoparticle concentration correction function, which quantifies the regulatory effect of concentration on phase equilibrium:

$$f(c)=\begin{cases}1+k\cdot c, c\le 1000\text{mg/L}\\ 1+k\cdot\dfrac{1000}{c}, c\ge 1000\text{mg/L}\end{cases} \quad (5)$$

where c is the nanoparticle injection concentration, mg/L; k is the experimental fitting coefficient, which is determined by history matching as $k=2.3\times10^{-4}\text{L/mg}$ in this model.

2.3.2 Phase equilibrium constraints

For the oil-aqueous two-phase system, the mole fractions of components in each phase must satisfy the normalization condition. Combined with the definition of the K, the phase equilibrium constraints are derived as follows:

$$\sum_{i=1}^{2}x_i=1\ ,\ \sum_{i=1}^{2}w_i=1 \quad (6)$$

$$x_i=K_i^{ow}\cdot w_i\ \ (i=1,2) \quad (7)$$

where $i=1$ represents the crude oil component, $i=2$ represents the aqueous component.

2.3.3 Phase equilibrium correction for heterogeneous reservoirs

For the five-spot heterogeneous model (one injector and four producers), considering the influence of inter-well permeability differences on nanoparticle migration, a permeability correction factor $g(k)$ is introduced to optimize the phase equilibrium equation. El-Amin and Mahmoud (2014) supplemented this by incorporating buoyancy, capillary forces, and Brownian diffusion into their numerical model, which better describes nanoparticle transport and retention in mixed-wet porous media.

$$K_i^{ow}(p,T,c,k)=\frac{a_i}{p}\cdot\exp\left(-\frac{b_i}{T}\right)\cdot f(c)\cdot g(k) \quad (8)$$

where k is the reservoir permeability, mD; $g(k)=0.85+0.15\cdot\lg\left(\dfrac{k}{100}\right)$ (applicable for $100\le k\le 5000\text{mD}$).

3 Model construction

The basic parameters of the model are set with reference to actual reservoir conditions of low-permeability sandstone reservoirs in the Ordos Basin and relevant literature data (Mahmud et al., 2021; Shao et al., 2023), as shown in Table 1. The model adopts a non-uniform grid with dimensions of 20×20×5 (x×y×z), with grid refinement near the wellbore to improve the calculation accuracy of fluid flow around the well. The residual oil saturation (0.43) refers to the experimental data of sandstone reservoirs by Mahmud et al. (2021), the formation water salinity (10,000 mg/L) complies with the common industrial oilfield water quality standard, and the nanoparticles selected are industrially used modified silicon-based nanoparticles (particle size: 10-30 nm).

Key parameters such as relative permeability curves and capillary pressure curves are calibrated using core flooding experimental data (ASTM D7370 standard). The experimental core samples

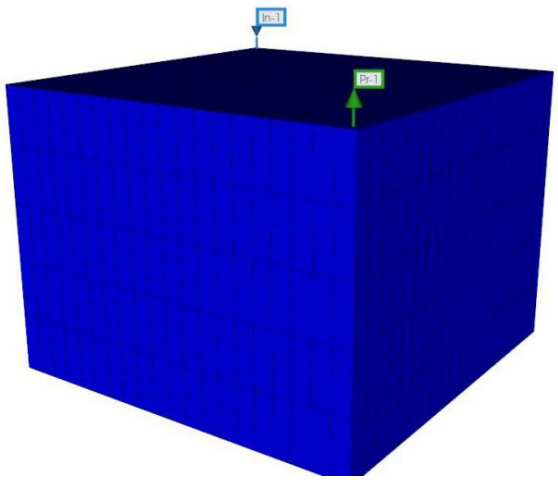

Fig.1 3D Model diagram

are consistent with the reservoir lithology (sandstone), with porosity of 0.22-0.28 and permeability of 100-1000 mD. The model is verified by comparing the simulation results with experimental recovery rates, with a relative error of less than 5%, confirming the reliability of the model. The 3D model diagram is presented in Figure 1.

Table 1 Basic model parameters

Model Parameter	Value	Model Parameter	Value
Grid number	20×20×5	Porosity	0.25
Initial oil saturation	0.65	Residual oil saturation	0.43
Reference temperature	65°C	Irreducible water saturation	0.35
Reference pressure	3994.3 psi	Water salinity	10000 mg/L
Water density	1000 g/cm3	Oil density	980 g/cm³

4 Results

As a core analysis tool in the field of numerical simulation, sensitivity analysis accurately identifies key parameters that significantly affect model output and deeply reveals the intrinsic behavioural laws of the research system by systematically adjusting input parameters and tracking the response characteristics of output results. This section focuses on key operational parameters adjustable in field development and basic reservoir physical parameters, conducting sensitivity analysis based on the single-injection single-production homogeneous model and the single-injection four-production heterogeneous model, respectively.

4.1 Single-injection single-production homogeneous model

4.1.1 Study on the effect of injection rate

Based on CMG-STARS, injection rate simulations were carried out under different nanoparticle concentrations (0, 500 mg/L, 1000 mg/L, 1500 mg/L, 2000 mg/L), with five gradient rates set: 400, 600, 800, 1000, and 1200 m^3/d. Each rate-concentration combination was subjected to long-term dynamic simulation to capture the entire oil displacement process.

The effects of injection rate under different nanoparticle concentrations are shown in Figure 2. Analysis indicates that at low concentrations (≤500 mg/L), nanoparticles have limited impact on fluid properties, and the injection rate mainly affects displacement power. High rates can push the oil-water interface faster but tend to cause uneven displacement; at high concentrations (≥1500 mg/L), high rates may exacerbate particle aggregation, affecting their migration and action in pores. An injection rate of 800 m^3/d balances displacement efficiency and sweep uniformity, achieving the optimal recovery rate for all concentrations, with an increase of 3.5%-7.6% compared to the 400 m^3/d rate. Diasty and VÚRUP (2025) further expanded this analysis by combining concentration (3 wt.%), slug size, and injection rate optimization, showing that matching slug size to injection rate can reduce nanoparticle loss while maintaining recovery rate.

4.1.2 Study on the effect of injection timing

Injection timing is directly related to the contact timing, action duration, and sweep range of displacement fluid and crude oil, exerting a profound impact on the final recovery rate and economic benefits. Based on fixed key parameters such as nanoparticle concentration (1000 mg/L), injection rate (800 m^3/d), and reservoir permea-

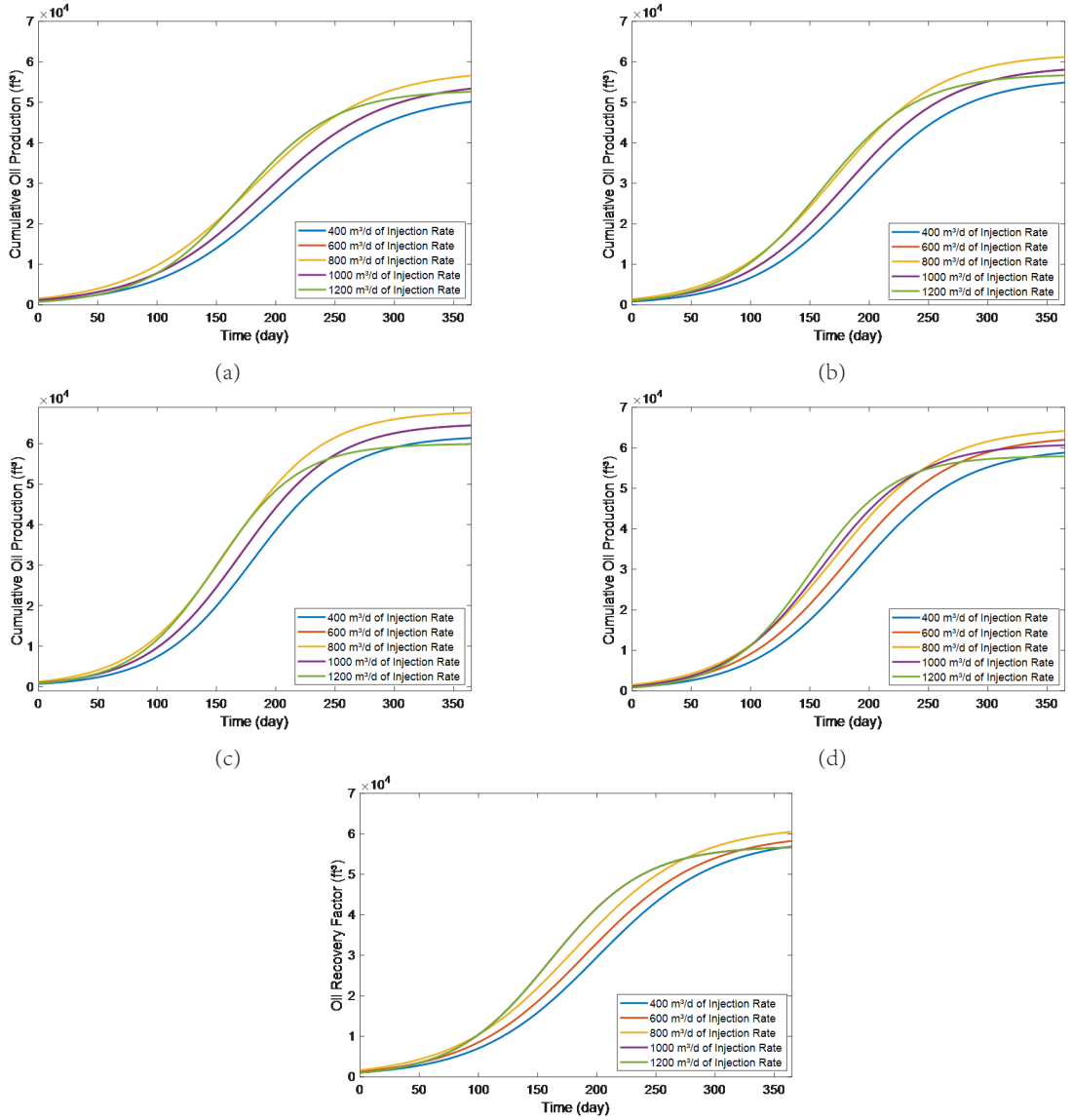

Fig.2 Cumulative oil production under different injection rates and nanoparticle concentrations

bility (1000 mD), only the nanoparticle injection timing was changed, and five simulation schemes were designed to quantitatively analyse the dynamic oil displacement process under different injection timings.

The gradient design of injection timing is shown in Table 2, and the simulation results are presented in Figure 3. Analysis shows that injecting nanofluid when water flooding reaches a 45% recovery rate achieves synergistic enhancement of water flooding and nanoparticle flooding, with a final recovery rate of 65.8%, which is 6.2% higher than that of early water flooding injection and 4.8% higher than that of late water flooding injection. When injected in the early stage of water flooding, nanoparticles are prone to rapid breakthrough with the water flow, failing to fully exert plugging

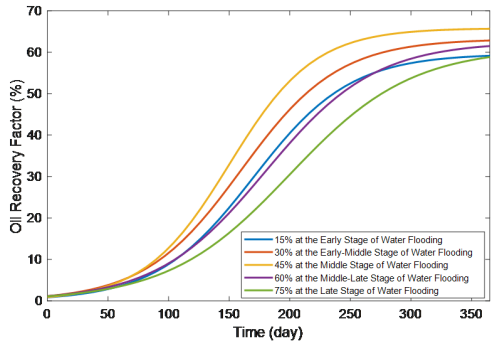

Fig.3 Oil recovery factor changes under different injection timings

and oil washing effects; when injected in the late stage of water flooding, most of the movable oil in the reservoir has been produced, leaving limited room for efficiency improvement by nanoparticle flooding.

Table 2 Gradient design of injection timing

Description of Injection Timing	Recovery Rate
Early stage of water flooding	15%
Early-middle stage of water flooding	30%
Middle stage of water flooding	45%
Middle-late stage of water flooding	60%
Late stage of water flooding	75%

4.1.3 Study on the effect of homogeneous permeability

As a core parameter characterizing the characteristics of reservoir fluid migration channels, homogeneous permeability directly determines the migration rate, retention law of nanoparticles in porous media, and displacement fluid sweep efficiency. Using the "control variable method," this study fixed key parameters such as nanoparticle concentration (1000 mg/L), injection rate (800 m^3/d), and injection timing (water flooding 45% stage), only changing the homogeneous permeability value, and set five gradient schemes covering different reservoir types with varying development difficulties.

The gradient permeability schemes are shown in Table 3, and the simulation results are presented in Figure 4. Analysis indicates that the higher the permeability, the faster the initial cumulative oil production increases, and the higher the final cumulative oil production. At a permeability of 5000 mD (ultra-high permeability), the cumulative recovery rate reaches 72.3%, which is 12.8% higher than that of the 100 mD (ultra-low permeability) reservoir. High permeability reduces the retention loss of nanoparticles in porous media, extends the interaction time between particles and crude oil, and expands the displacement fluid sweep volume, thereby significantly improving the recovery rate; in low-permeability reservoirs, nanoparticle migration is hindered, and they are prone to retention in the near-wellbore zone, making it difficult to exert full-scale displacement effects.

Table 3 Five gradient permeability schemes

Permeability Grade	Value/mD
Ultra-low permeability	100
Low permeability	300
Medium permeability	1000
High permeability	2000
Ultra-high permeability	5000

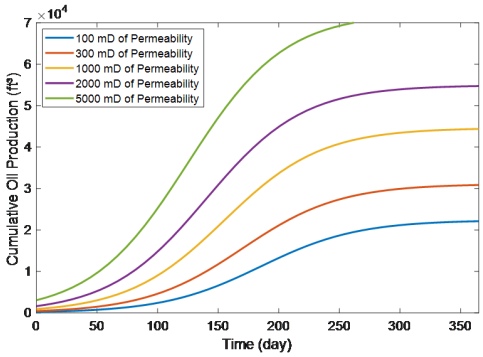

Fig.4 Cumulative oil production comparison under five permeability levels

4.1.4 Study on the effect of homogeneous porosity

To systematically explore the regulatory law of reservoir storage space characteristics on nanoparticle oil displacement efficiency, this section takes homogeneous porosity as the core variable, selects representative gradient values within the common reservoir porosity range to set four groups of control experiments, and fixes key parameters such as reservoir homogeneous permeability (1000 mD), nanoparticle injection concentration (1000 mg/L), injection rate (800 m^3/d), and injection timing (water flooding 45% stage).

The gradient porosity schemes are shown in Table 4, and the simulation results are presented in Figure 5. Analysis shows that the higher the porosity, the larger the storage space, the wider the sweep range of nanoparticles and displacement fluid, and the higher the recovery rate. At a porosity of 0.35 (high porosity group), the final recovery rate reaches 70.1%, which is 9.5% higher than that of the 0.2 (low porosity group). High porosity reduces the risk of particle aggregation and pore plugging, while providing more sufficient channels for crude oil flow; in low-porosity reservoirs, space constraints easily lead to particle aggregation, affecting displacement efficiency.

Table 4 Four gradient porosity schemes

Porosity Grade	Value
Low porosity group	0.2
Base control group	0.25
Medium-high porosity group	0.3
High porosity group	0.35

4.1.5 Study on the effect of different nanoparticle injection concentration

The nanoparticle injection concentration gradient was set as 0 (pure water flooding control group), 500, 1000, 1500 and 2000 mg/L. The variation laws of recovery rate and injection pressure under different concentrations were analysed through simulation to explore the mechanism of concentration on oil displacement efficiency.

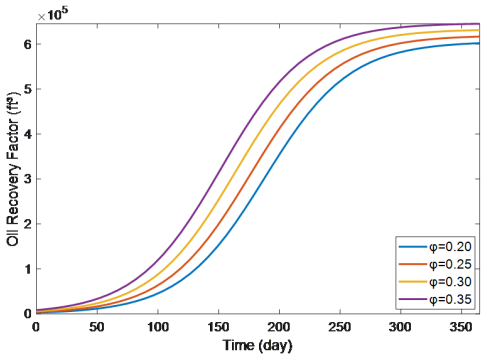

Fig.5 Oil recovery factor comparison under different porosities

The simulation results are presented in Figure 6. Analysis shows that a nanoparticle concentration of 1000 mg/L is optimal, with a corresponding final recovery rate of 65.8%, which is 13.6% higher than that of pure water flooding. When the concentration is lower than 1000 mg/L, the number of particles is insufficient to effectively reduce interfacial tension and plug high-permeability channels; the recovery rate at 500 mg/L is only 60.2%, which is 5.6% lower than that at 1000 mg/L. When the concentration is higher than 1000 mg/L, the van der Waals force between particles increases, leading to aggregation, and the pore plugging rate increases to 8.3%. The recovery rates at 1500 and 2000 mg/Ldecrease to 63.5% and 61.7%, respectively, which are lower than the optimal concentration. Rezaei, Jafari, and Rahimi (2020) also reported similar findings in their numerical study of random pore porous media, noting that smaller nanoparticle diameters (2nm) and moderate volume fractions (5vol.%) optimize recovery, while excessive concentration exacerbates pore blocking.

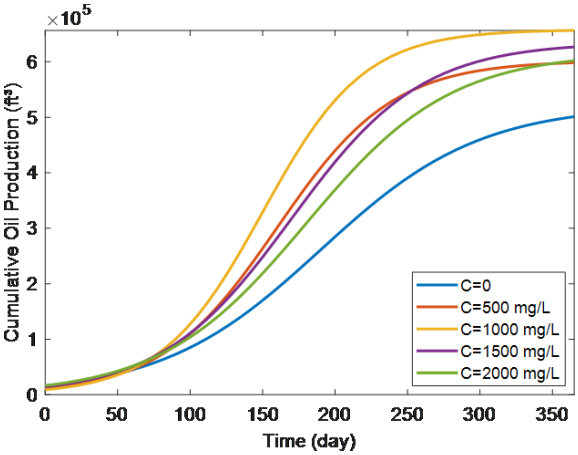

Fig.6 Oil recovery factor changes under different injection timings

4.2 Single-injection four-production heterogeneous model

4.2.1 Model construction

Based on the permeability statistical data of an actual sandstone reservoir (mean value 1000 mD, coefficient of variation 0.8), a heterogeneous field was generated, including high-permeability channels (permeability 2000-5000 mD), low-permeability zones (100-300 mD), and permeability transition zones (300-2000 mD). The injection well is in the centre, and four production wells are deployed in different permeability zones. The well location coordinates and corresponding permeability intervals are shown in Table 5, and the permeability distribution contour map is presented in Figure 7.

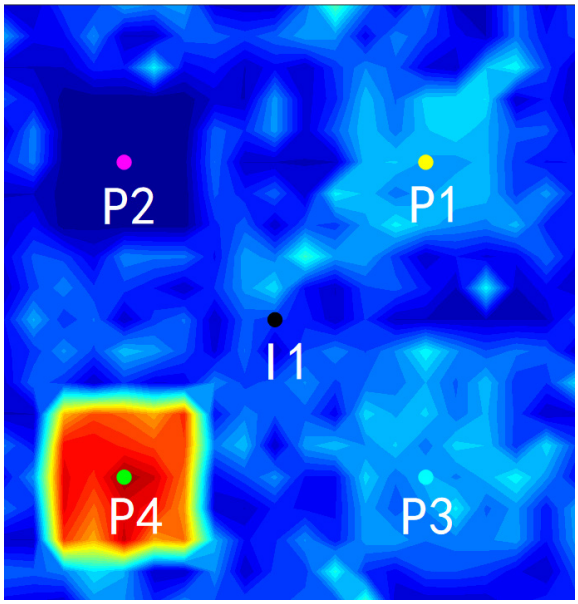

Fig.7 Permeability distribution contour map of the heterogeneous model

4.2.2 Analysis of oil displacement efficiency

The simulation adopted the optimal injection parameter combination (nanoparticle concentration 1000 mg/L, injection rate 800 m^3/d, injection at the water flooding 45% stage). The comparison results of oil production, water cut, and recovery rate of the four production wells are shown in Figure 8.

Analysis indicates that the difference in inter-well permeability distribution plays a dominant role in nanoparticle oil displacement efficiency. For Producer P3 in the low-permeability zone, nanoparticles form effective plugging in the near-wellbore zone, forcing displacement fluids

Table 5 Well locations and permeability information of the single-injection four-production model

Well Type	Well Number	Coordinates	Permeability Interval	Permeability Type
Inject	I1	(10,10,3)	1000 mD	Medium permeability
Produce	P1	(5,5,3)	2000-5000 mD	High-permeability channel
Produce	P2	(5,15,3)	300-2000 mD	Permeability transition zone
Produce	P3	(15,5,3)	100-300 mD	Low-permeability zone
Produce	P4	(15,15,3)	300-2000 mD	Permeability transition zone

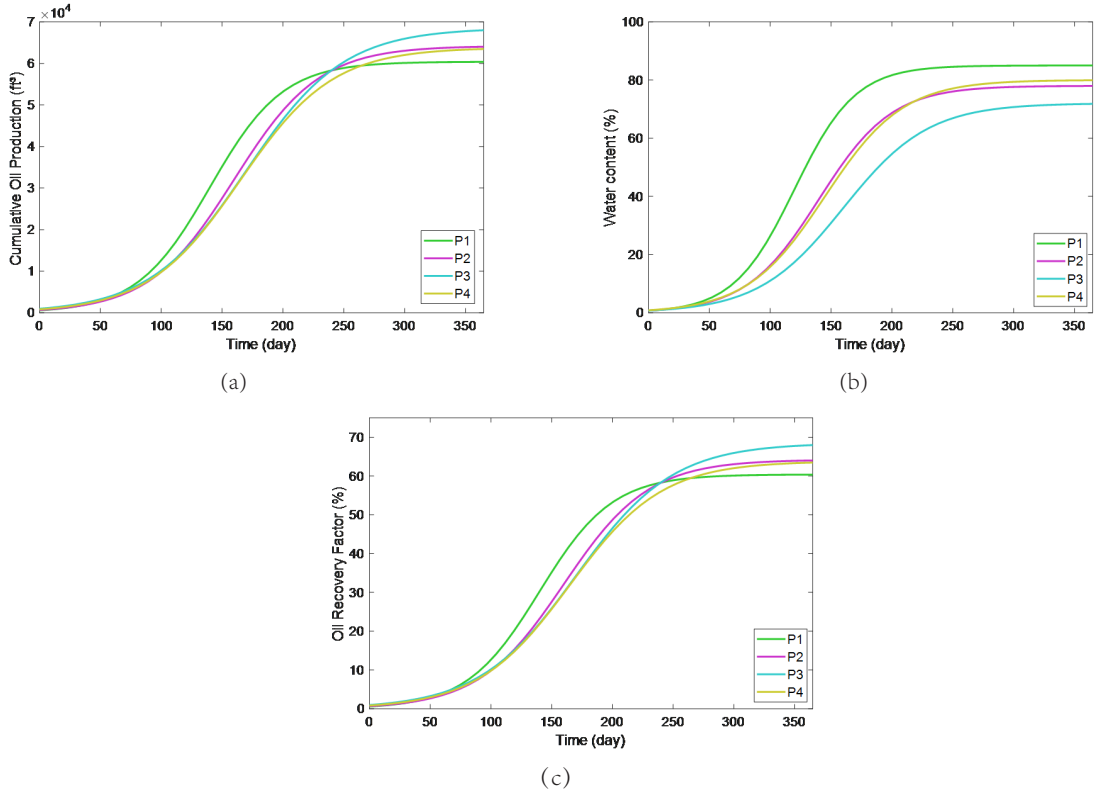

Fig.8 Comparison of cumulative oil production/water content/oil recovery factor of four production wells

to divert to undeveloped crude oil zones, resulting in a recovery rate of 68.5% with an increase of 10.2%. For Producer P1 in the high-permeability channel, nanoparticles migrate quickly with less retention, making early breakthrough prone, leading to a rapid increase in water cut; the recovery rate is only 60.4% with an increase of 4.3%. The oil displacement efficiency of Producers P2 and P4 in the permeability transition zone is between the two, showing a stepwise recovery rate change characteristic, with recovery rates of 64.2% and 63.8%, and increases of 7.0% and 6.6%, respectively.

4.2.3 Analysis of inter-well interference

The influence of the distance between the injection well and different production wells, as well as permeability channels on displacement fluid distribution, was analysed. As illustrated in Figure 9 and Figure 10, the results show that the resistance between Producer P1 (connected to high-permeability channels) and the injection well is small, so displacement fluid arrives first, and the nanoparticle breakthrough time is 140 days earlier than that of Producer P3 (low-permeability zone)—this difference in breakthrough time is clearly reflected in the comparative analysis of Figure 10. Meanwhile, Figure 9 quantitatively presents the correlation between inter-well interference coefficients and recovery rate loss: the inter-well interference coefficient between Producers P1 and P2 is 0.35, resulting in a 3.2% decrease in the recovery rate of Producer P2 compared to the non-interference scenario; the inter-well interference coefficient between Producers P3 and P4 is 0.18, with a relatively small interference impact (only a 0.8% recovery rate loss), which is consistent with the weak positive correlation trend shown in Figure 9.zone)—this difference

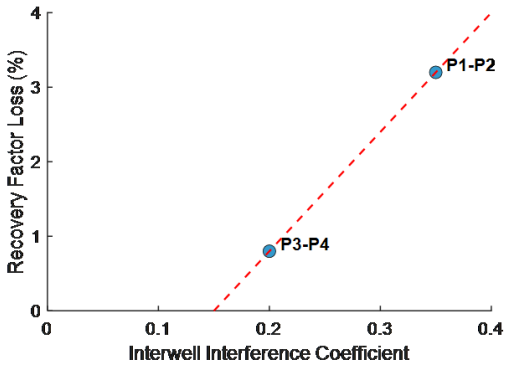

Fig.9 Relationship between inter-well interference coefficient and recovery rate loss

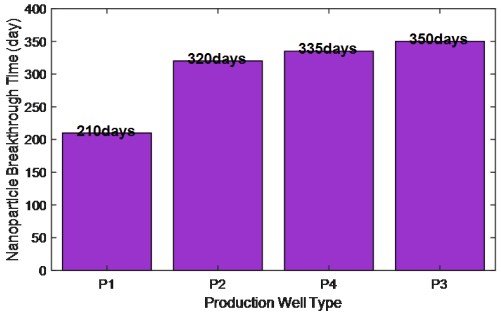

Fig.10 Comparison of nanoparticle breakthrough time among different production wells

in breakthrough time is clearly reflected in the comparative analysis of Figure 10. Meanwhile, Figure 9 quantitatively presents the correlation between inter-well interference coefficients and recovery rate loss: the inter-well interference coefficient between Producers P1 and P2 is 0.35, resulting in a 3.2% decrease in the recovery rate of Producer P2 compared to the non-interference scenario; the inter-well interference coefficient between Producers P3 and P4 is 0.18, with a relatively small interference impact (only a 0.8% recovery rate loss), which is consistent with the weak positive correlation trend shown in Figure 9.

5 Discussion

This study focuses on modified silicon-based nanoparticle EOR in low-permeability and heterogeneous reservoirs, constructing a multi-scenario numerical model and conducting systematic parameter sensitivity analysis. The key findings are discussed in depth below:

(1) A 3D two-phase two-component numerical model for nanoparticle EOR was successfully constructed based on CMG-STARS. Grid sensitivity analysis to determine the optimal grid density of 20×20×5, the model can accurately describe fluid migration laws and nanoparticle action processes and can handle complex reservoir conditions such as single-well homogeneous and multi-well heterogeneous reservoirs.

(2) The optimal intervals and quantitative effects of core parameters were clarified. The combination of nanoparticle concentration 1000 mg/L, injection rate 800 m3/d, and injection at the water flooding 45% stage is optimal, achieving a cumulative recovery rate of 65.8%, which is 13.6% higher than that of pure water flooding. The recovery rates of reservoirs with high permeability (5000 mD) and high porosity (0.35) are 12.8% and 9.5% higher than those of ultra-low permeability (100 mD) and low porosity (0.2) reservoirs, respectively.

(3) In heterogeneous reservoirs, the difference in inter-well permeability distribution dominates oil displacement efficiency. The recovery rate increase of production wells in low-permeability zones (10.2%) is 2.4 times that of production wells in high-permeability channels (4.3%). High-permeability channels are prone to early nanoparticle breakthrough, while low-permeability zones achieve efficient displacement due to plugging effects, and permeability transition zones show a stepwise recovery rate characteristic.

This study's findings directly guide the field application of modified silicon-based nanoparticle EOR, particularly the design and optimization of injection schemes for low-permeability heterogeneous reservoirs with significant permeability differences. Quantified optimal parameter combinations and regulatory mechanisms help cut field pilot costs and boost technology promotion success.

6 Appendix

Sensitivity coefficient calculation formula:

$$S_i = \frac{R_{\max,i} - R_{\min,i}}{\sum_{j=1}^{n}\left(R_{\max,j} - R_{\min,j}\right)}$$

Where S_i is the sensitivity coefficient of the i-th parameter; $R_{\max,i}$ and $R_{\min,i}$ are the maximum and minimum recovery rates under different levels of the i-th parameter, respectively; n is the number of parameters.

Wettability alteration efficiency calculation formula:

$$\eta_w = \frac{\theta_0 - \theta_n}{\theta_0 - 90^\circ}$$

Where η_w is the wettability alteration efficiency; θ_0 is the original contact angle; θ_n is the contact angle after nanofluid treatment.

Acknowledgement

None.

Funding Statement

This research did not receive any specific grant from funding agencies in the public, commercial, or not-for-profit sectors.

Author Contributions

The author confirms sole responsibility for the following: study conception and design, data-collection, analysis and interpretation of results, and manuscript preparation.

Availability of Data and Materials

The raw data generated in this study can be obtained from the corresponding author upon reasonable request. The reason for the temporary non-publication of data is to protect commercial secrets.

Conflicts of Interest

No potential conflict of interest was reported by the author(s).

ORCID

Chen Zhang: https://orcid.org/0009-0001-9987-5645

Xiang Rao: https://orcid.org/0000-0002-1856-1581

References

[1] Ackah, I., & Kizys, R. (2015). Green growth in oil producing African countries: A panel data analysis of renewable energy demand. Renewable and Sustainable Energy Reviews, 50, 1157-1166.

[2] Li, W., Zhang, H., & Wang, L. (2025). Experimental Study on a Nanoemulsion for EOR in High-Temperature, High-Salinity, Low-Permeability Reservoirs and Its Performance. ACS Omega, 10(49), 49136-49147.

[3] Agista, M. N., Guo, K., & Yu, Z. (2018). A state-of-the-art review of nanoparticles application in petroleum with a focus on enhanced oil recovery. Applied sciences, 8(6), 871.

[4] Agi, A., Junin, R., & Gbadamosi, A. (2018). Mechanism governing nanoparticle flow behaviour in porous media: insight for enhanced oil recovery applications. International Nano Letters, 8, 49-77.

[5] Druetta, P., & Picchioni, F. (2019). Polymer and nanoparticles flooding as a new method for Enhanced Oil Recovery. Journal of petroleum science and engineering, 177, 479-495.

[6] Lv, B., Sun, P., Wu, Y., Yang, Z., Liu, P., Wang, C., & Liu, Q. (2023). Study and Application of Oily Sludge Profile Control Technology in Heavy Oil Reservoir. Energies, 16(13), 5064.

[7] Singh, R., & Mohanty, K. K. (2015). Synergy between nanoparticles and surfactants in stabilizing foams for oil recovery. Energy & Fuels, 29(2), 467-479.

[8] El-Diasty, A. I., & Aly, A. M. (2015, September). Understanding the mechanism of nanoparticles applications in enhanced oil recovery. In SPE North Africa technical conference and exhibition (p. D021S009R004). SPE.

[9] Rao, X., Cheng, L., Cao, R., Jia, P., Liu, H., & Du, X. (2022). A meshless numerical modeling method for fractured reservoirs based on extended finite volume method. SPE Journal, 27(6), 3525-3542.

[10] Rao, X., Li, L., Jia, P., & Cheng, L. (2023a). A Novel Projection-based Embedded Discrete Fracture Model (pEDFM) for Anisotropic Two-phase Flow Simulation Using Hybrid of Two-point Flux Approximation and Mimetic Finite Difference (TPFA-MFD) Methods. Journal of Computational Physics, 482, 112736.

[11] Rao, X., Jia, P., Cheng, L., & Li, L. (2024a). A first streamline-based simulation method within the projection-based embedded discrete fracture model (pEDFM). Computational Geosciences, 28(2), 1-18.

[12] Li, L., Rao, X., Jia, P., & Cheng, L. (2025). A Hybrid Method Combining Mimetic Finite Difference and Discontinuous Galerkin for Two-Phase Reservoir Flow Problems. International Journal for Numerical Methods in Fluids, 97(3), 484-502.

[13] Zhang, Y., Rao, X., Li, L., & Jia, P. (2025). The First Application of Quantum Computing Algorithm in Streamline-Based Simulation of Water-Flooding Reservoirs. Quantum Engineering, 7(1), 015002.

[14] Rao, X., Cheng, L., Jia, P., & Li, L. (2023b). A generic workflow of projection-based embedded discrete fracture model for flow simulation in porous media. Computational Geosciences, 27(4), 1-16.

[15] Rao, X., Cheng, L., Jia, P., & Li, L. (2024b). A modified projection-based embedded discrete fracture model (pEDFM) for practical and accurate numerical simulation of fractured reservoir. Journal of Petroleum Science and Engineering, 232, 111654.

[16] Lu, T., Li, Z., Zhou, Y., & Zhang, C. (2017). Enhanced oil recovery of low-permeability cores by SiO2 nanofluid. Energy & fuels, 31(5), 5612-5621.

[17] Khalilnezhad, A., Rezvani, H., Talebi, A., Ganji, P., Puntervold, T., & Riazi, M. (2023). Improved oil recovery in carbonate cores using alumina nanoparticles. Energy & Fuels, 37(16), 11765-11775.

[18] Mohanty, U. S., Awan, F. U. R., Ali, M., Aftab, A., Keshavarz, A., & Iglauer, S. (2021). Physicochemical characterization of zirconia nanoparticle-based sodium alginate polymer suspension for enhanced oil recovery. Energy & Fuels, 35(23), 19389-19398.

[19] Khoramian, R., Ramazani SA, A., Hekmatzadeh, M., Kharrat, R., & Asadian, E. (2019). Graphene oxide nanosheets for oil recovery. ACS Applied Nano Materials, 2(9), 5730-5742.

[20] Yang, D., Peng, X., Peng, Q., Wang, T., Qiao, C., Zhao, Z., ... & Zeng, H. (2022). Probing the interfacial forces and surface interaction mechanisms in petroleum production processes. Engineering, 18, 49-61.

[21] Chen, Y., Liu, J., & Zhang, Y. (2025). Mechanistic Insights into Nanoparticle-Modified Polymer Flooding for Enhanced Oil Recovery. Langmuir, 41(31), 12089-12101.

[22] Guzei, D. V., Minakov, A. V., Pryazhnikov, M. I., & Ivanova, S. V. (2022). Numerical investigation of enhanced oil recovery from various rocks by nanosuspensions flooding. Journal of Applied and Computational Mechanics, 8(1), 306-318.

[23] Sepehri, M., Moradi, B., Emamzadeh, A., & Mohammadi, A. H. (2019). Experimental study and numerical modeling for enhancing oil recovery from carbonate reservoirs by nanoparticle flooding. Oil & Gas Science and Technology - Revue d'IFP Energies nouvelles, 74(1), 1-14.

[24] Zhang, Y., Li, J., & Wang, H. (2019). The effect of nanoparticles on wettability alteration for enhanced oil recovery: micromodel experimental studies and CFD simulation. Petroleum Science (China University of Petroleum, Beijing), 16(5), 1123-1132.

[25] Ivanov, A., Petrov, P., & Smirnov, V. (2025). A Systematic Microfluidic Study of the Use of Diluted Silica Sols to Enhance Oil Displacement. Scientific Reports, 15(1), 17892.

[26] Cao, L. (2015). A Field-scale simulation of the reversible nanoparticle adsorption for enhancing oil recovery using hydrophilic nanofluids. University of Louisiana at Lafayette.

[27] Ortiz Maestre, D. P. (2017). Mechanistic modeling of nanoparticle-stabilized supercritical CO2 foams and its implication in field-scale EOR applications.

[28] Kumar, N., Pal, N., & Mandal, A. (2021). Nanoemulsion flooding for enhanced oil recovery: Theoretical concepts, numerical simulation and history match. Journal of Petroleum Science and Engineering, 202, 108579.

[29] Mahmud, H. B., Tan, B. C., Giwelli, A., Al-Rubaye, A. F., & Shafiq, M. U. (2021). Numerical analysis of SiO2-SDS surfactant effect on oil recovery in sandstone reservoirs. Energy Geoscience, 2(4), 238-245.

[30] Jafarbeigi, E., Salimi, F., Kamari, E., & Mansouri, M. (2022). Effects of modified graphene oxide (GO) nanofluid on wettability and IFT changes: Experimental study for EOR applications. Petroleum Science, 19(4), 1779-1792.

[31] Shao, W., Yang, J., Wang, H., Chang, J., Wu, H., & Hou, J. (2023). Recent research progress on imbibition system of nanoparticle-surfactant dispersions. Capillarity, 8(2), 34-44.

[32] Bahadori, N. (2024). Experimental and Numerical Investigation of Droplet Dynamics in Microscale Systems: The Influence of Surfactants and Nanoparticles on Environmental Applications (Master's thesis, Louisiana Tech University).

[33] Garcia, R., Martinez, L., & Rodriguez, S. (2025). Numerical study of the mechanisms of nano-assisted foam flooding in porous media as an alternative to gas flooding. PLOS ONE, 20(5), e030907739.

[34] Wang, C., Li, H., & Zhang, Q. (2024). Comprehensive study of nano-composite polymer flooding under reservoir conditions: New insights into enhanced oil recovery. Journal of Petroleum Science and Engineering, 232, 111876.

[35] El-Amin, M. F., & Mahmoud, M. (2014). Enhanced Oil Recovery by Nanoparticles Injection: Modeling and Simulation. ResearchGate.

[36] Diasty, A. I., & VÚRUP, S. (2025). Optimization of Nanofluid Systems for Enhanced Oil Recovery: Analysis of Concentration, Slug Size, and Injection Rates. VÚRUP Research Journal, 18(1), 45-62.

[37] Rezaei, M., Jafari, M., & Rahimi, M. (2020). Numerical Investigation of Controllable Parameters Effect on Nanofluid Flooding in a Random Pore Generated Porous Medium. Iranian Journal of Chemistry and Chemical Engineering, 39(2), 113-126.